NUCLEAR INSTRUMENTS AND METHODS 126 (1975) 49–55; © NORTH-HOLLAND PUBLISHING CO.

SUB-PICOSECOND LIFETIMES FROM DOPPLER-SHIFT ATTENUATION MEASUREMENTS FOLLOWING (α,2p) AND (α,pn) REACTIONS ON ^{54}Fe IN SINGLES EXPERIMENTS

J. URBON, D. G. SARANTITES and L. L. RUTLEDGE, Jr.

*Department of Chemistry, Washington University, St. Louis, Missouri 63130, U.S.A.**

Received 26 February 1975

A procedure is described by which the Doppler-shift attenuation technique is extended to measurement of nuclear-level lifetimes from singles experiments following two-nucleon emitting reactions. It is shown that in reactions such as (α,pn) and (α,2p) it is possible to obtain sub-picosecond lifetimes from the careful measurement at several bombardment energies of the line shapes and centroid shifts of γ-rays near and above the threshold for the levels of interest. The values of (100 ± 15) fs, (580 ± 60) fs, and (180 ± 30) fs, (490 ± 50) fs were obtained for the mean lifetimes of levels at 3638.1, 4180.4 keV in ^{56}Co, and 3755.8, 5255.5 keV in ^{56}Fe, respectively.

1. Introduction

The Doppler-shift attenuation (DSA) technique has been employed rather extensively in recent years by many investigators (see, for example, refs. 1–10) for obtaining nuclear-level lifetimes in the time range 10^{-14}–10^{-11} s. In the simplest application of this technique the state under investigation is populated in very short time ($\ll 10^{-14}$ s) by a nuclear reaction. The state of interest decays then by γ-ray emission at a later measurable time. The observed shifts depend on the distribution of the recoil velocities at the time of emission. The collection of nuclei which slow down in a given medium give a spectrum of shifts, the details of which depend on the slowing-down process and the lifetime of the decaying state. With the exception of singles observation near the threshold for the formation of a state or of coincidence experiments in reactions of the type (x,y) where the initial recoil velocity is defined by the reaction kinematics, all singles measurements[7]) give line shapes and shifts that depend on the respective recoil distribution. Furthermore, in more complex reactions of the type (α, 2n), (α, pn), etc., two additional complications arise. The first stems from the more complex kinematics due to several outgoing particles, thus making it practically impossible to define the recoil direction and energy in a particle vs γ-ray coincidence arrangement. The second and most severe complication arises in many instances from the complexity of the mode of formation of the state of interest, which in most cases may proceed via a cascade of known or unknown γ-ray transitions, involving states either in the bound region or in the unbound yrast-cascade region. In order to make possible the extraction of very short ($\leqslant 10^{-12}$ s) mean lifetimes one is forced to simplify the mode of formation of the states of interest. This in principle should be possible near the threshold for the state. The latter, however, presents obvious experimental difficulties stemming from small cross sections near the threshold.

It is the purpose of this paper to present some results on lifetimes extracted via the DSA technique in singles experiments by analyzing the Doppler shifts and line shapes of γ-rays observed in the reactions (α, 2p) and (α, pn) on ^{54}Fe at a series of α-bombardment energies. It is shown that sub-picosecond τ values can be extracted for high-spin states from such measurements.

2. Experimental procedures

In this work we have selected for careful study the α-particle-induced reactions on ^{54}Fe in the energy range 18–30 MeV. This choice was prompted by a previous detailed study of the mechanism of these reactions[11]) and by an independent study[12]) of the feeding times for states in ^{61}Cu populated by the ^{58}Ni(α, p) reaction at 20 MeV. The results of Sarantites, Barker, and Lu[12]) for the feeding times in ^{61}Cu showed that feeding times shorter than 0.5 ps may be expected in this region.

The α-beams required were obtained from the Washington University cyclotron.

2.1. Detection equipment and methods of measurement

For singles γ-ray spectrometry a 5.6% efficient

* Work supported in part by the U.S. Atomic Energy Commission under Contracts no. AT(11-1)-1530 and AT(11-1)-1760.

[compared to a 7.6-cm × 7.6-cm NaI(Tl) detector at 25 cm for a 1332 keV γ-ray] Ge(Li) detector with a full width at half maximum of 1.20 and 2.17 keV at 122 and 1332 keV, respectively, was used. This detector was operated in an anti-Compton arrangement[13]) which was located on an angular-correlation table that allowed spectra to be taken between 0° and 90° to the beam. A peak-to-Compton ratio of 100:1 for the 1274.51 keV γ-ray of ^{22}Na was obtained in this arrangement. In the present experiments the beam was stopped in a strip of lead sheet. Good collimation of the spectrometer permitted shielding of the γ-rays from the prompt reactions in Pb for detection angles down to 20° relative to the beam. For energies in excess of $\approx$24 MeV considerable neutron background was observed, due to reactions induced in the Pb beam stop. Calibration peaks were introduced in most of the spectra by counting in the presence of sources of ^{57}Co, ^{207}Bi, ^{22}Na,

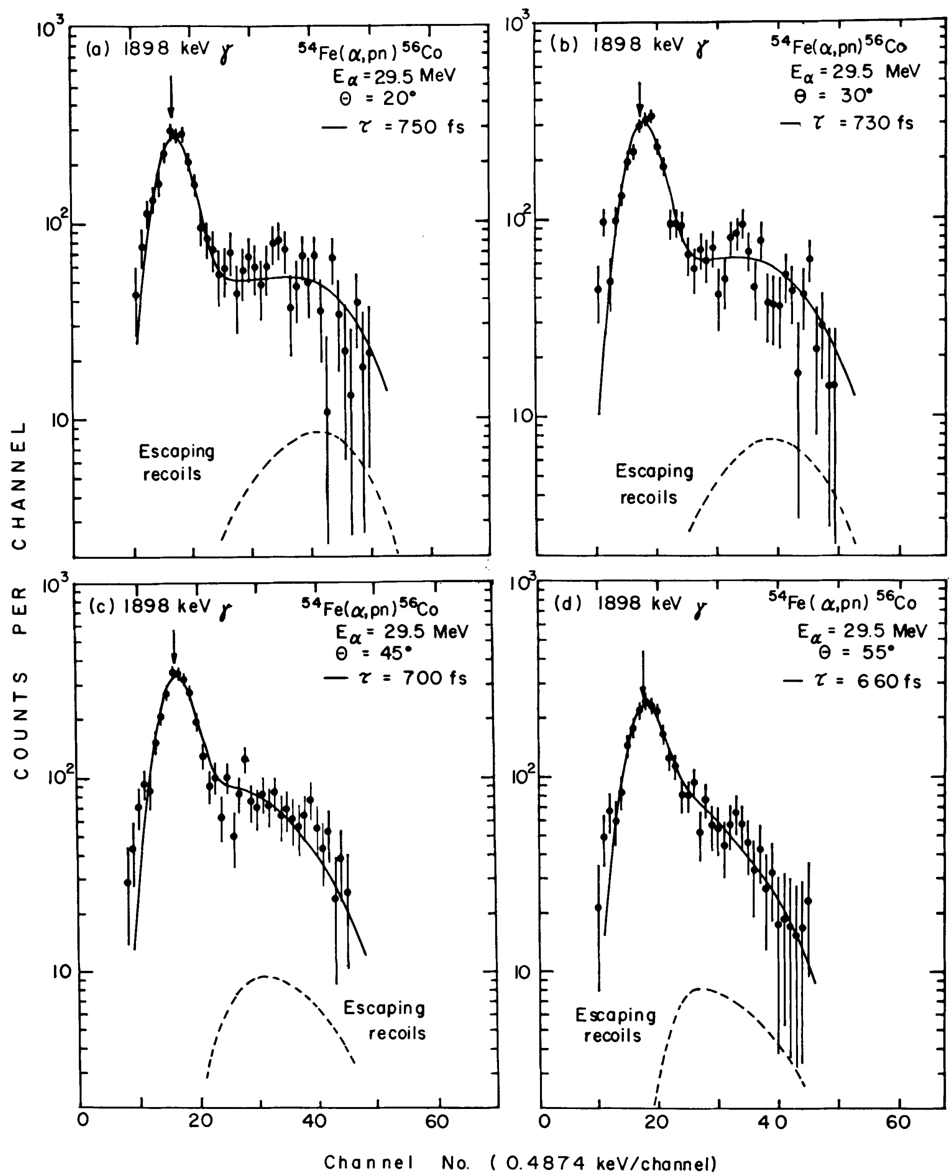

Fig. 1. Comparison of the calculated line shapes for the 1898 keV γ-ray in ^{56}Co with experimental data obtained in singles measurements at 20°, 30°, 45°, and 55° to the beam direction following the ^{54}Fe(α,pn)^{56}Co reaction at 29.5 MeV. The lifetimes that gave the minimum χ^2 are also given. The calculated shapes include corrections for the escaping recoils and for observed feeding from higher-lying states (see text).

^{137}Cs, ^{54}Mn, and ^{60}Co. These sources were prepared thin, and were mounted in front of the collimator of the anti-Compton spectrometer outside the lead shield.

The targets employed were 4.0 mg/cm^2 Fe self-supporting foils enriched to 97.12% in mass 54.

For data collection a 4096-channel pulse-height analyzer was used which was interfaced to a PDP 8/L computer.

2.2. Analysis of the observed Doppler shifts

The observed Doppler shifts were analyzed both by the line-shape and by the centroid-shift techniques. The detailed method employed in this work has been described in ref. 7. Here we need only to comment in some detail on the aspects characteristic of reactions involving two-nucleon emission.

First it should be mentioned that for Co and Fe nuclei recoiling into Fe as stopping medium the stopping powers $f_n = f_e = 0.84$ deduced[7]) for Cu ions stopping in Ni were used. These values are the adjustment factors for the nuclear and electronic stopping-power theory of Lindhard, Scharf, and Schiøtt[14]), as defined in ref. 7.

The effect of the reaction kinematics on the initial recoil distribution $d\sigma(\theta_R)/d\Omega$ which enters in eq. (4) of ref. 7 will be considered next. The additional uncertainties from emission of more than one nucleon are expected to introduce some error in the analysis. An estimate of the upper limit of maximum angle of the recoil cone can be obtained in the di-nucleon limit. In this limit both nucleons were assumed to be emitted as one particle of mass number $A = 2$ and carrying all the available kinetic energy.

A somewhat more realistic approach for estimating the recoil distribution was also employed in this work. An estimate of the most probable energy for the emitted protons in the (α, 2p) and (α, pn) reactions on ^{54}Fe was obtained from the measurements and from the statistical-model calculations of Lu[11]). Thus, the most probable energy for one proton was kept constant, and for each possible angle the energy and momentum conservation was applied to the emission of the second nucleon. In this case the nucleon emission was treated as isotropic in the center-of-mass system and properly converted to the laboratory system. This yielded a more realistically weighted recoil cone. It is interesting to note that the recoil energies differed only by a few percent from the di-nucleon approximation.

The recoil-γ angular-correlation effects were treated in the manner described in ref. 7.

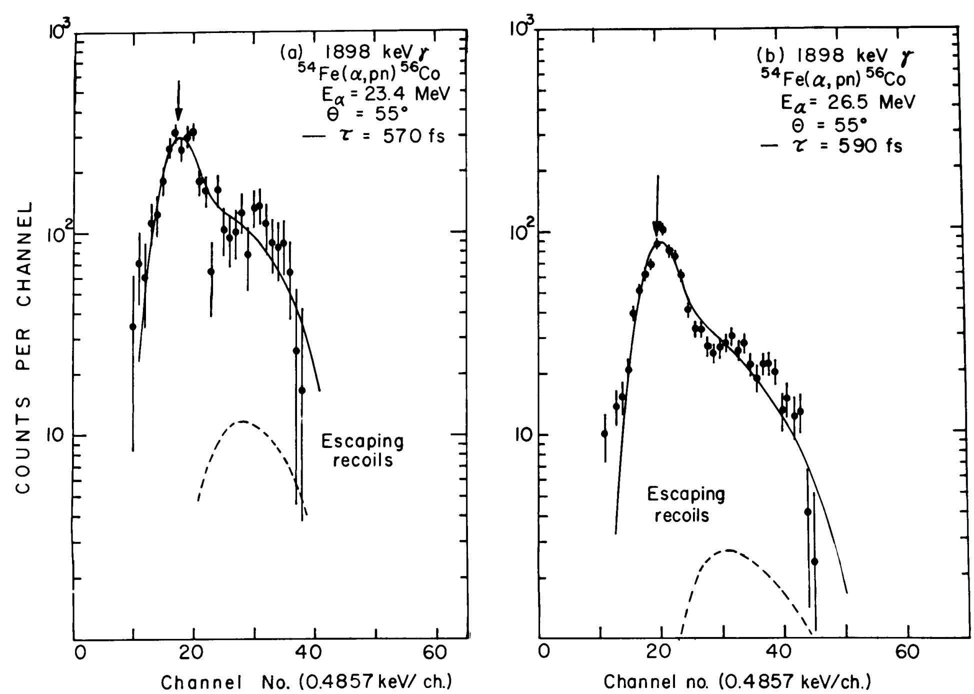

Fig. 2. Comparison of the calculated line shapes for the 1898 keV γ-ray with experimental data obtained in singles experiments at 55° to the beam direction following the ^{54}Fe(α,pn)^{56}Co reaction at 23.4 and 26.5 MeV. The lifetimes quoted correspond to shapes giving the minimum χ^2 value.

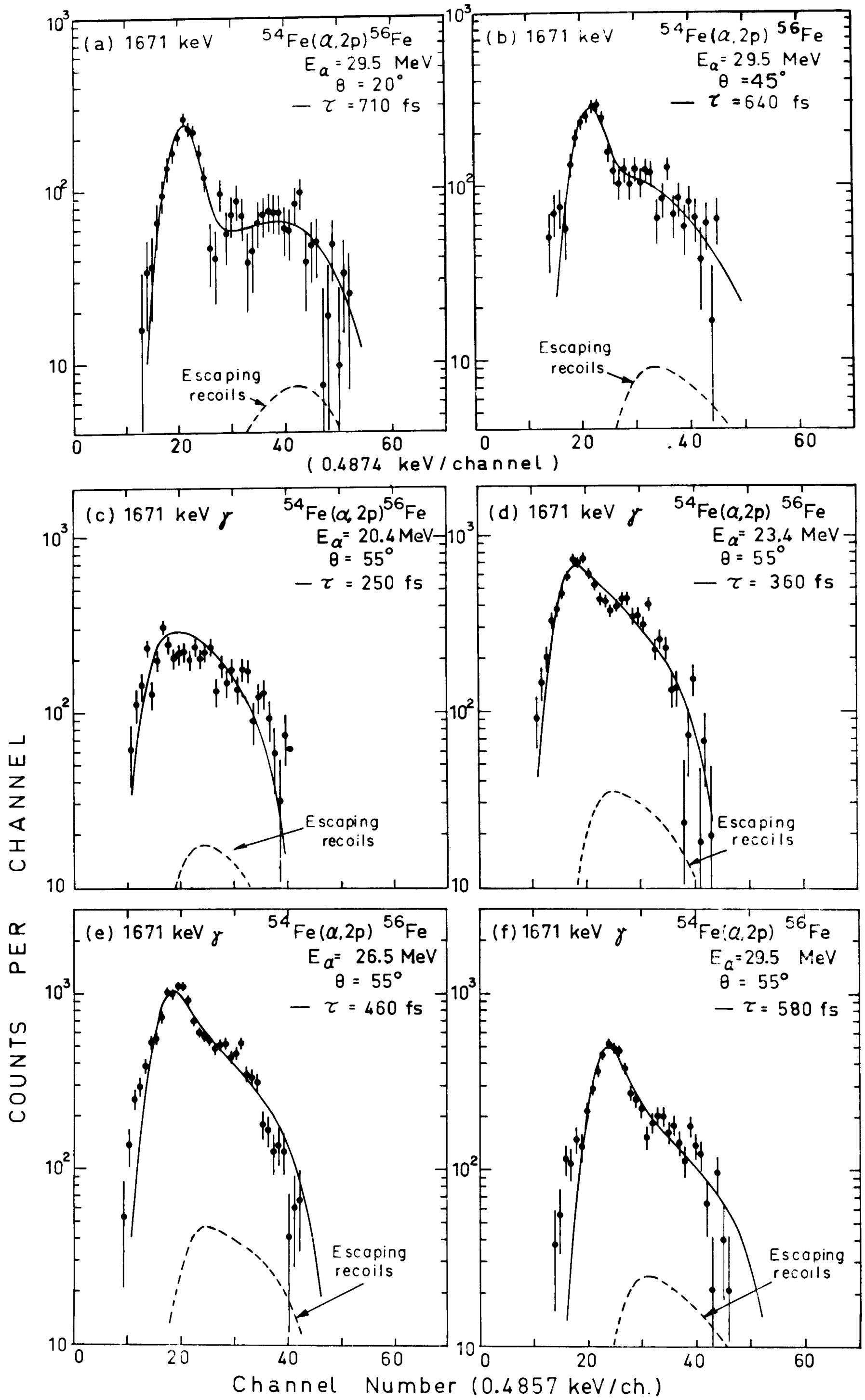

Fig. 3. Comparison of the calculated line shapes for the 1671 keV γ-ray in ^{56}Fe with experimental data obtained in singles experiments at 20° and 45° following the $^{54}Fe(\alpha,2p)^{56}Fe$ reaction at 29.5 MeV [frames (a) and (b)]. The lower four frames show the calculated and experimental line shapes observed at 55° for the four α-bombardment energies indicated. No feeding from higher-lying states was observed in this case.

3. Results and discussion

In this work we present some results from selected E2 and primarily M1 transitions from high-spin states in ^{56}Co and ^{56}Fe reached by the (α,pn) and (α,2p) reactions on ^{54}Fe in the energy range 21–30 MeV. Complete angular distributions and Doppler-shift measurements were taken at 30 MeV of incident energy at angles of 20°, 30°, 45°, 60°, 70°, 75°, and 90° to the beam direction. Line-shape measurements were taken at (20.4±0.7), (23.4±0.6), (26.5±0.6), and (29.5±0.6) MeV at 55° to the beam direction.

In fig. 1 are shown the line shapes obtained for the 1898-keV transition between the levels[15]) at 4180 (9_1^+)→2283 (7_1^+) keV in ^{56}Co. The experimental results in fig. 1 are compared with the fitted theoretical line shapes indicated by the solid lines. At 29.5 MeV this level was found to receive 25% of its yield via a higher-lying state, which in turn was found to have an effective lifetime of 0.21 ps at this energy. The effect of such a feeding has been included in the calculated line shapes.

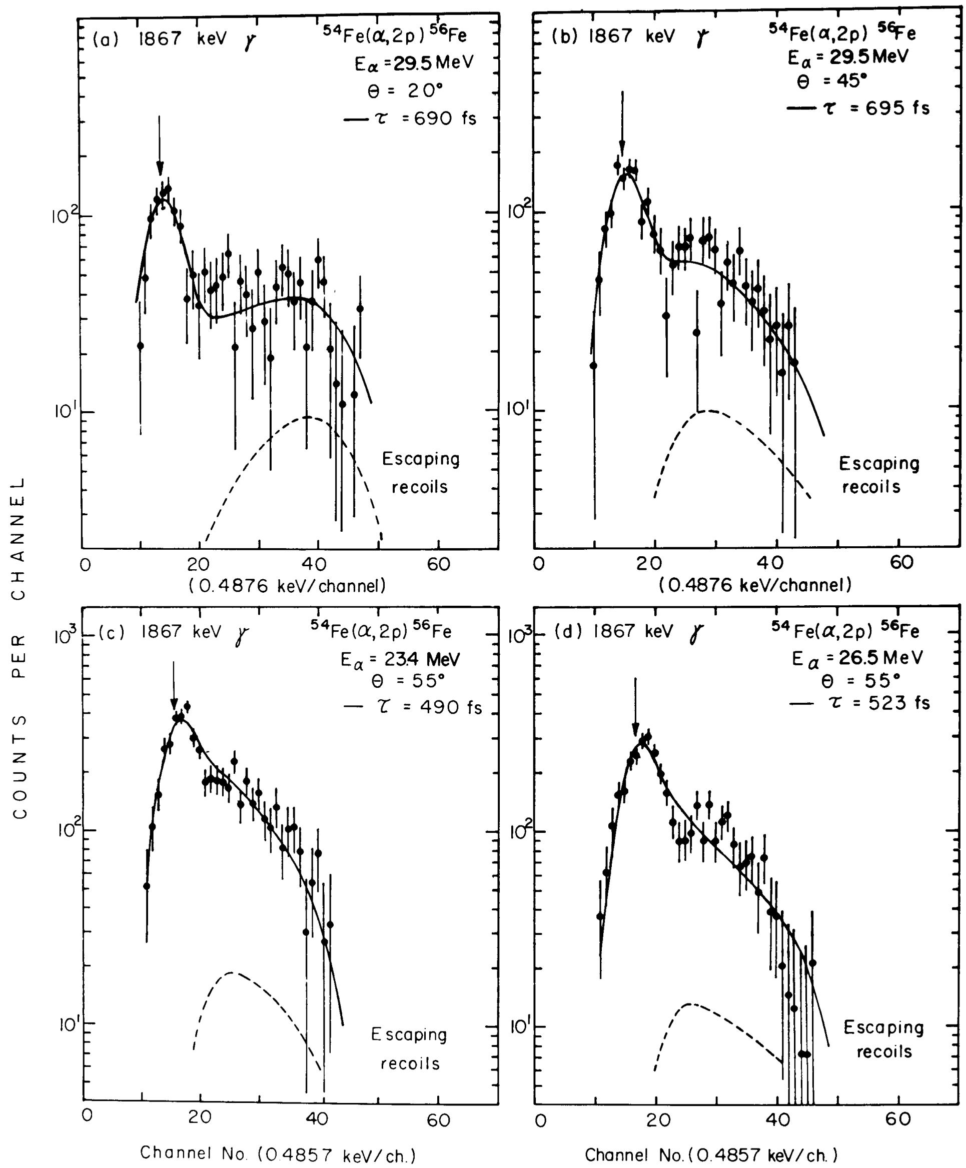

Fig. 4. Comparison of calculated and measured line shapes for the 1867 keV γ-ray in ^{56}Fe following the ^{54}Fe(α,2p) reaction at the indicated angles and α-bombardment energies. No feeding from higher-lying states was observed. The extracted lifetimes corresponding to minimum χ^2 are also given.

Feeding, however, via other unobserved non-yrast transitions from bound or unbound states in ^{56}Co were not included in the calculated shapes. It is seen that the observed line shapes are nicely reproduced also at higher detection angles. For this transition a small systematic decrease is observed in the lifetimes that give the lowest χ^2 value to the data. For the same transition in fig. 2 are shown the observed shifts at 23.4 and 26.5 MeV of incident energy. The shapes of fig. 2 were observed at 55°. The calculated shapes shown as solid lines in fig. 2 include the effect of feeding from a higher-lying level with feeding fraction of 6.5 and 19.4% and effective lifetimes of 0.073 and 0.208 ps for the two energies of 23.4 and 26.5 MeV, respectively.

In contrast to the case of the 1898-keV E2 transition in ^{56}Co, which showed an effective level lifetime with a small decrease with decreasing projectile energy, we show next in fig. 3 the observed line shapes for the 1671-keV transition between the levels[15,16]) at 3756 $(6_2^+) \rightarrow 2085\ (4_1^+)$ keV in ^{56}Fe. The calculated shapes shown in fig. 3 have been obtained assuming only one component in the decay process since no feeding from other higher-lying bound states was observed. The top frames (a) and (b) of fig. 3 show the shapes observed at 20° and 45° to the beam direction. The lifetimes that gave the minimum χ^2 value from shapes at different angles agree within experimental error. For this transition a pronounced dependence of the observed shift on the bombardment energy is seen. This is reflected in a rather rapidly decreasing effective lifetime with decreasing bombardment energy.

Finally in fig. 4 are shown selected observed shapes for the 1867-keV transitions in ^{56}Fe. This transition was found[15,16]) also to have an E2 character[15]), and connects the states 5256 $(8_1^+) \rightarrow 3388\ (6_1^+)$ in ^{56}Fe. Furthermore, no feeding was observed[15]) from higher-lying bound states. Figs. 4(a) and 4(b) show the line shapes observed for this transition at 20° and 45° to the beam direction from the $^{54}Fe(\alpha, 2p)$ reaction at 29.5 MeV. It is seen that these line shapes are well reproduced by the calculation and for the angles indicated show consistent lifetimes at minimum χ^2. In figs. 4(c) and 4(d) are shown the fitted line shapes for the 1867-keV transition in ^{56}Fe at 23.4 and 26.5 MeV of α-bombardment energy.

In the determination of the lifetimes reported here, the observed centroid shifts were also analyzed. As expected, these results also gave lifetimes consistent with values obtained from the analysis of the line shapes. In fig. 5 are shown the centroid shift results from the 29.5-MeV experiment. The slopes were obtained by least-squares fits to the data and are given in the figure in keV.

In table 1, we summarize the lifetime information from this work. The first two columns of table 1 give the level and the transition energy used in the measurements. The third column gives the incident α-particle energy, and the fourth column gives the effective mean lifetimes obtained as a weighted average of the values from the analysis of the line shapes and centroid shifts

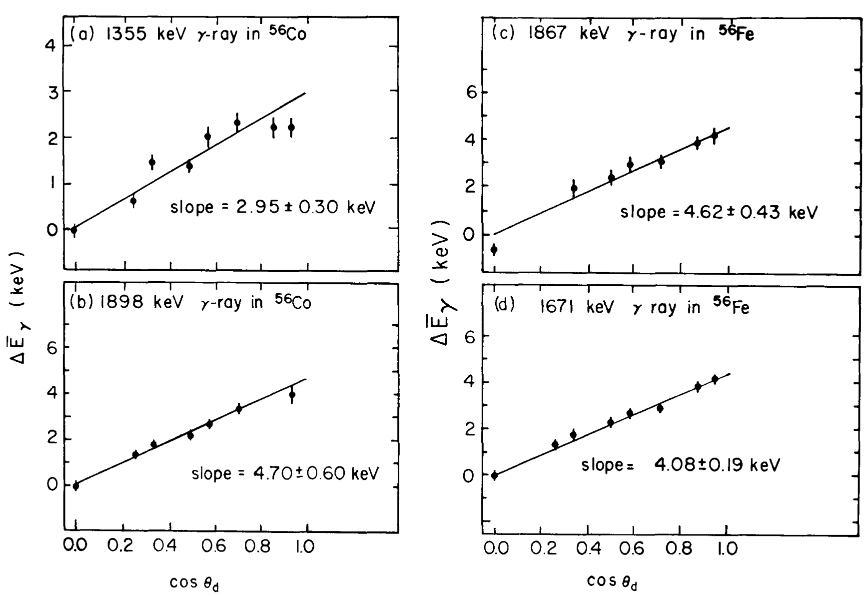

Fig. 5. Plots of the centroid shift in keV for the indicated γ rays in ^{56}Co and ^{56}Fe observed in singles measurements vs cos θ. The least-squares slopes for a straight-line fit to the data are also given in keV.

TABLE 1

Summary of the deduced mean lifetimes of some high-spin states in ^{56}Co and ^{56}Fe populated in the (α,pn) and (α,2p) reactions on ^{54}Fe in the energy range 20.4–29.5 MeV.

Level (keV)		Transition (keV)	E_α (MeV)	Effective τ (fs)[a]		Proposed level τ (fs)	
^{56}Co	3638.1	1355.4	20.4	120	*40*	100	*15*
			23.4	175	*31*		
			26.5	270	*28*		
			29.5	540	*140*		
	4180.4	542.0, 1898.0	20.4	582	*100*	580	*60*
			23.4	577	*88*		
			26.5	617	*54*		
			29.5	750	*60*		
^{56}Fe	3755.8	1670.8	20.4	218	*30*	180	*30*
			23.4	360	*40*		
			26.5	428	*47*		
			29.5	720	*85*		
	5255.5	1867.1	20.4	500	*85*	490	*50*
			23.4	474	*62*		
			26.5	532	*60*		
			29.5	725	*86*		

[a] Values obtained as weighted averages of the results from the line-shape fits and the centroid shifts.

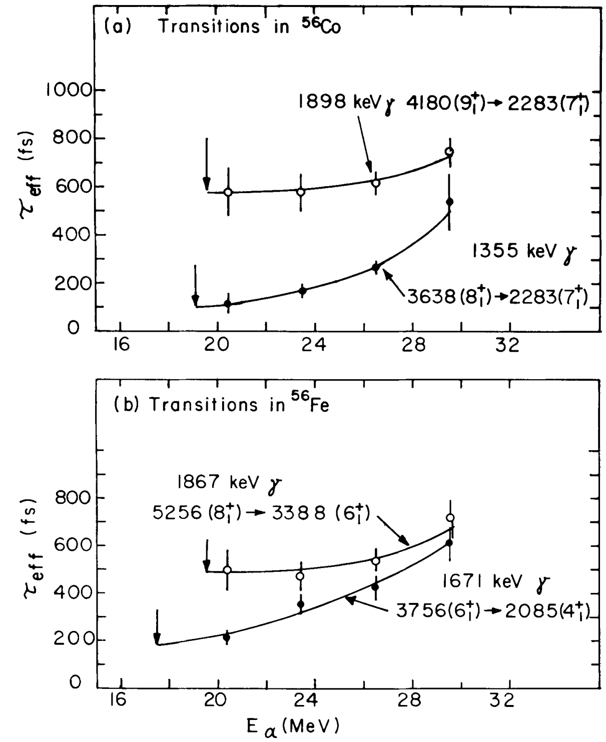

Fig. 6. Plots of the extracted effective mean lifetimes vs α-bombardment energy for the transitions in ^{56}Co and ^{56}Fe indicated. The vertical arrows show the projectile energies below which the γ rays in question could not be observed. The proposed mean lifetimes for the levels analyzed were obtained by extrapolation to these bombardment energies.

at the bombardment energies indicated. Although these values have been corrected for reduced shifts from observed feeding via higher-lying states, they still show a gradual increase in lifetime with increasing bombardment energy. This reflects the effect of some unobserved feeding from higher-lying states or most likely from cascades in the unbound region. For the 5256-keV level in ^{56}Fe the mean lifetimes given are weighted averages from two transitions at 542 and 1898 keV which were shown[15,16]) to deexcite this level.

The effective mean lifetimes given in table 1 are plotted vs the incident α-particle energy in fig. 6. The calculated threshold energies for the formation of the levels of interest are shown by vertical arrows in fig. 6. It is seen that the effective lifetimes essentially level off as the threshold values are approached.

We wish to thank the personnel of the Washington University Cyclotron Laboratory for their assistance during the course of these experiments. The cooperation of the staff of the Washington University Computing Facilities is also appreciated.

References

1) E. K. Warburton, J. W. Olness and A. R. Poletti, Phys. Rev. **160** (1967) 938.
2) A. E. Blaugrund, Nucl. Phys. **88** (1966) 501.
3) P. A. Assimakopoulos, T. Becker, C. Moazed and D. M. Van Patter, Nucl. Phys. **A180** (1972) 131.
4) W. M. Curnie, L. G. Earwaker and J. Martin, Nucl. Phys. **A135** (1969) 325.
5) M. Bister, A. Antilla, M. Piiparinen and M. Viitasula, Phys. Rev. **C3** (1971) 1972.
6) C. Broude, P. Engelstein, M. Popp and P. N. Tandon, Phys. Letters **398** (1972) 185.
7) E. J. Hoffman, D. M. Van Patter, D. G. Sarantites and J. H. Barker, Nucl. Instr. and Meth. **109** (1973) 3.
8) D. G. Sarantites, J. H. Barker, N.-H. Lu, E. J. Hoffman and D. M. Van Patter, Phys. Rev. **C8** (1973) 629.
9) J. H. Barker and D. G. Sarantites, Phys. Rev. **C10** (1974) 1407.
10) R. A. Braga and D. G. Sarantites, Phys. Rev. **C10** (1974) 2109.
11) N.-H. Lu, Ph. D. Thesis (Washington University, St. Louis, Missouri, 1974) unpublished.
12) D. G. Sarantites, J. H. Barker and N.-H. Lu, Phys. Rev. **C9** (1974) 603.
13) M. E. Phelps, D. G. Sarantites and W. G. Winn, Nucl. Phys. **A149** (1970) 647.
14) L. Lindhard, M. Scharff and H. E. Schiott, Kgl. Danske Videnskab. Selskab, Mat.-Fys. Medd. **33**, no. 14 (1963).
15) J. Urbon and D. G. Sarantites (1974) unpublished.
16) A. R. Poletti, B. A. Brown, D. B. Fossan and E.K. Warburton, Phys. Rev. **C10** (1974) 2329.